J Mater Sci (2006) 41:6622–6630
DOI 10.1007/s10853-006-0201-x

Numerical prediction of damage in composite structures from soft body impacts

Alastair F. Johnson · Martin Holzapfel

Published online: 8 August 2006

Abstract The paper summarises recent progress on materials modelling and numerical simulation of soft body impact damage in fibre reinforced composite aircraft structures. The work is based on the application of finite element (FE) analysis codes to simulate damage in composite shell structures under impact loads. Composites ply damage models and interply delamination models have been developed and implemented in commercial explicit FE codes. Models are discussed for predicting impact loads on aircraft structures arising from deformable soft bodies such as gelatine (synthetic bird) and ice (hailstone). The composites failure models and code developments are briefly summarised and applied in the paper to numerical simulation of synthetic bird impact on idealised composite aircraft structures.

Introduction

The paper reviews recent progress on materials modelling and numerical simulation of soft body impact on fibre reinforced composite structures. To reduce certification and development costs, computational methods are required by the aircraft industry able to predict structural integrity of composite structures under high velocity impacts from soft or deformable bodies such as birds, hailstones and tyre rubber. Key issues are the development of suitable constitutive laws for modelling composites in-ply and delamination failures, determination of composites parameters from high rate materials tests, materials laws for soft body impactors, and the efficient implementation of the materials models into FE codes. These problems involve both multi-scale and multi-physics modelling techniques which are discussed in the paper. The multi-scale aspects arise because impact damage is localised and requires fine scale modelling of delamination and ply damage at the micromechanics level, whilst the structural length scale is much larger. The multi-physics aspects arise in fluid-structure interactions when soft bodies such as gelatine (substitute bird) or ice (hailstones) flow extensively on impact with the structure and require fluid modelling techniques.

The work is based on the application of explicit FE codes to simulate composite shell structures under high velocity impact. Improved composites ply damage and interply delamination models have been developed based on a continuum damage mechanics (CDM) formulation from Ladevèze and his co-workers [1] and implemented in a commercial explicit FE code [2]. The CDM ply failure model uses three scalar damage parameters representing modulus reductions under different loading conditions due to microdamage in the ply, and the delamination model requires two interface fracture energy parameters. The paper summarises the CDM failure models for composites, discusses how damage parameters are determined from measured damage evolution laws and then describes recent work on impact simulation of damage to composite structures from soft deformable impactors. Soft body projectiles such as gelatine or ice are highly deformable and flow on impact, spreading the impact load and causing a pressure pulse in the structure. Modelling techniques are described based on an elastic–plastic materials law with equation of

A. F. Johnson (✉) · M. Holzapfel
German Aerospace Center (DLR), Institute of Structures and Design, Stuttgart, Germany
e-mail: alastair.johnson@dlr.de

state [3], combined with a discrete element particle mesh which replaces the highly distorted solid elements. The code developments are applied in the paper to a design study for a novel composite wing leading edge (LE) concept structure, in which a high tenacity polyethylene fibre fabric (Dyneema) membrane is laminated into the carbon/epoxy LE shell. Simulation results show that on bird impact the carbon/epoxy plies fracture whilst the PE fabric ply undergoes large membrane deformations, which prevent penetration by the bird and absorb a significant part of the bird kinetic energy in agreement with structural tests. This LE concept demonstrates the feasibility of hybrid composite laminate architectures designed with dual functions of high stiffness and enhanced impact resistance. The FE modelling studies of the complex damage behaviour shows the potential of simulation tools for future application in design concept studies for novel composites aircraft structures subjected to severe loads.

Damage modelling in composite laminates

Polymer composites exhibit a range of failure modes: matrix cracking, transverse ply cracks, fibre fracture, fibre pull-out, microbuckling, interply delamination etc, which are initiated at the micro level and can be modelled by micromechanics techniques at length scales governed by fibre diameters. The length scale for aircraft structural analysis is in metres, with shell element size for crash or impact simulations in FE analyses measured in cms. Meso-scale models based on continuum damage mechanics are the link in the FE code between composites micro- and macroscales. CDM provides a framework within which in-ply and delamination failures may be modelled. In the work described here the composite laminate is modelled by layered shell elements or stacked shells with a cohesive interface which may fail by delamination. The shells are composed of composite plies which are modelled as a homogeneous orthotropic elastic or elastic–plastic damaging material whose properties are degraded on loading by microcracking prior to ultimate failure. In its present form, the model assumes that intraply damage acts independently from interply damage hence the ply and delamination models are described separately here. Micromechanics studies now show that delamination in UD composites is initiated by ply cracking. However, the general CDM formulation is general enough for coupling between ply damage and delamination parameters to be included in future developments.

Elastic ply damage mechanics model

A CDM formulation is used in which ply degradation parameters are internal state variables which are governed by damage evolution equations. Constitutive laws for orthotropic elastic materials with internal damage parameters are described in [1], and take the general form

$$\boldsymbol{\varepsilon}^{\mathrm{e}} = \boldsymbol{S}\boldsymbol{\sigma}, \tag{1}$$

where $\boldsymbol{\sigma}$ and $\boldsymbol{\varepsilon}^{\mathrm{e}}$ are vectors of stress and elastic strain, and $\boldsymbol{S}$ is the elastic compliance matrix. For shell elements a plane stress formulation with orthotropic symmetry axes (x_1, x_2) is required. The in-plane stress and strain components are

$$\boldsymbol{\sigma} = (\sigma_{11}, \sigma_{22}, \sigma_{12})^T \quad \boldsymbol{\varepsilon}^{\mathrm{e}} = (\varepsilon^{\mathrm{e}}_{11}, \varepsilon^{\mathrm{e}}_{22}, 2\varepsilon^{\mathrm{e}}_{12})^T. \tag{2}$$

Using a strain equivalent damage mechanics formulation, the elastic compliance matrix $\boldsymbol{S}$ may then be written:

$$\boldsymbol{S} = \begin{pmatrix} 1/E_1(1-d_1) & -\nu_{12}/E_1 & 0 \\ -\nu_{12}/E_1 & 1/E_2(1-d_2) & 0 \\ 0 & 0 & 1/G_{12}(1-d_{12}) \end{pmatrix}. \tag{3}$$

The compliance matrix has three scalar damage parameters d_1, d_2, d_{12} and four initial or ''undamaged'' elastic constants: the Young's moduli in the principal orthotropy directions E_1, E_2, the in-plane shear modulus G_{12}, and the principal Poisson's ratio ν_{12}. The damage parameters d_1, d_2, d_{12} have values $0 \leq d_i < 1$ and represent modulus reductions under different loading conditions due to microdamage in the material. For UD plies d_1 and d_2 are associated with damage or failure in fibre longitudinal and transverse directions, for fabric plies in the principal fibre directions, and d_{12} controls in-plane shear damage. In the general damage mechanics formulation ''conjugate forces'' or damage energy release rates Y_1, Y_2, Y_{12} are introduced corresponding to ''driving'' mechanisms for materials damage, and it is shown that with the compliance matrix (3) they take the form:

$$\begin{aligned} Y_1 &= \sigma_{11}^2/(2E_1(1-d_1)^2), \\ Y_2 &= \sigma_{22}^2/(2E_2(1-d_2)^2), \\ Y_{12} &= \sigma_{12}^2/(2G_{12}(1-d_{12})^2). \end{aligned} \tag{4}$$

The ply model is completed by assuming damage evolution equations in which the three ply damage parameters d_1, d_2, d_{12} are functions of Y_1, Y_2, Y_{12}. Specific forms for these functions are postulated based on study of ply specimen test data. The formulation of the damage evolution equations in the Ladevèze CDM models is physically based and allows generalisations to include features such as shear plasticity and rate dependence. Test data on unidirectional (UD) carbon fibre reinforced epoxy presented in [4] show that damage evolution equations for the transverse and shear damage d_2, d_{12} are coupled

through a linear dependence on $\sqrt{(Y_2)}$ and $\sqrt{(Y_{12})}$. Test data on carbon and glass fabric/epoxy materials [5] lead to damage evolution equations in which fibre tension/compression damage parameters d_1, d_2 are elastic damaging and linear in $\sqrt{(Y_1)}$ and $\sqrt{(Y_2)}$, respectively, but decoupled from elastic/plastic ply shear damage in which d_{12} is a nonlinear function of $\sqrt{(Y_{12})}$. Note that the further extension of the ply damage model (1)–(3) to include an irreversible plastic damage component is discussed further in [2, 4].

These ply damage models are available as global ply failure models in the explicit commercial FE code PAM-CRASH^{TM} [6]. In addition the code has alternative ''bi-phase ply models'' which are meso-scale damage models, in which the ply stiffness and strength are calculated by superimposing the effects of an orthotropic matrix and one or more fibre phases, each with its own damage function d. The compliance matrix again has the form (1) with the simplifying assumption that the orthotropic matrix phase has a single damage function acting on the stiffness constants which is assumed to be a function of the second strain invariant ε_{II}, or the effective shear strain. A bi-linear damage evolution equation is assumed for $d\ (\varepsilon_{II})$ after an initial elastic behaviour is exceeded. The fibre damage parameter is superimposed in the fibre directions to allow for fibre dominated failure mechanisms, where $d\ (\varepsilon_f)$ is a function of fibre strain ε_f. The PAM-CRASH^{TM} FE code contains bilinear 4-node quadrilateral isoparametric shell elements with uniform reduced integration in bending and shear. A Mindlin–Reissner shell formulation is used with a layered shell description to model a composite ply, a sublaminate or the complete laminate. In the composite layered shell element the stiffness properties of the plies are degraded, as defined by the ply model being used, until eventually a damaged shell element is eliminated from the computation when a chosen composites failure criterion such as maximum stress, maximum strain, effective shear strain, etc reaches a pre-defined critical value.

Delamination model

Delamination failures occur in composite structures under impact loads due to local contact forces in critical regions of load introduction and at free edges. They are caused by the low, resin dominated, through-thickness shear and tensile properties found in laminated structures. In composites delamination models [7], the thin solid interface is modelled as a sheet of zero thickness, across which there is continuity of surface tractions but jumps in displacements. The equations of the model are given here for the case of mode I tensile failure at an interface. Let σ_{33} be the tensile stress applied at the interface, u_3 the displacement across the interface, and k_3 the tensile stiffness. Following [8] an elastic damaging interface stress–displacement model is assumed:

$$\sigma_{33} = k_3(1-d_3)u_3,$$
$$d_3 = c_1(1-u_{30}/u_3), \quad \text{for } u_{30} \le u_3 \le u_{3m}, \tag{5}$$

with tensile damage parameter d_3, and $c_1=u_{3m}/(u_{3m}-u_{30})$. It can be verified that with this particular choice of damage function d_3, the stress–displacement function has the triangular form shown in Fig. 1, and u_{30}, u_{3m} correspond to the displacement at the peak stress σ_{33m} and at ultimate failure. The damage evolution constants are defined in terms of σ_{33m} and G_{IC}, the critical fracture energy under mode I interface fracture, by $u_{30} = \boldsymbol{\sigma}_{33m}/k_3$ and $u_{3m} = 2G_{IC}/\boldsymbol{\sigma}_{33m}$. From these expressions it can be shown that the area under the curve in Fig. 1 is equal to the fracture energy G_{IC}. This interface model therefore represents an initially elastic interface, which is progressively degraded after reaching a maximum tensile failure stress $\boldsymbol{\sigma_{33m}}$ so that the mode I fracture energy is fully absorbed at separation. For mode I interply failure the interface energy G_I, defined as

$$G_I = \int_0^{u_3} \sigma_{33}\mathrm{d}u_3, \tag{6}$$

is monitored and, if this is found to exceed the critical fracture energy value G_{IC}, then the crack is advanced. For mode II interface shear fracture a similar damage interface law to (5) is assumed, with equivalent set of damage constants, u_{130}, u_{13m} and critical fracture energy G_{IIC}. In general there will be some form of mixed mode delamination failure involving both shear and tensile failure. This is incorporated in the model by assuming a mixed mode failure condition, which for mode I/mode II coupling could be represented by an interface failure envelope:

$$\left(\frac{G_I}{G_{IC}}\right)^n + \left(\frac{G_{II}}{G_{IIC}}\right)^n = e_D < 1, \tag{7}$$

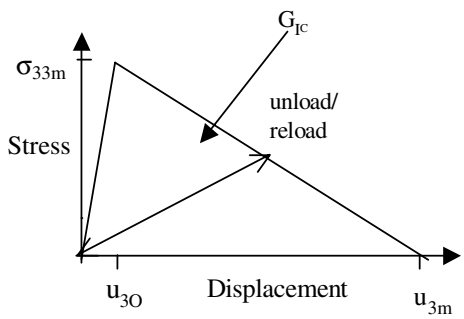

Fig. 1 Idealised mode I interface stress–displacement function

where G_I and G_{II} are the monitored interface strain energy in modes 1 and 2, respectively, G_{IC} and G_{IIC} are the corresponding critical fracture energies and the constant n is chosen to fit the mixed mode fracture test data. Typically n is found to between 1 and 2. Failure at the interface is imposed by degrading stresses when $e_D < 1$. When $e_D \geq 1$ in (7) there is delamination and the interface separates.

The delamination model is implemented in the PAM-CRASH^{TM} code, with the laminate modelled as a stack of shell elements. Each ply or sublaminate ply group is represented by a shell element and the individual sublaminate shells are connected together using a contact interface with an interface traction–displacement law. The interface is a contact constraint not an interface element in which a penalty force procedure is used to compute contact forces between adjacent shells. Contact may be broken when the interface energy dissipated reaches the mixed mode delamination energy criteria (7). This ''stacked shell'' approach is an efficient way of modelling delamination, with the advantage that the critical integration timestep is relatively large since it depends on the area size of the shell elements not on the interply thickness.

Modelling impact behaviour of soft body impactors

Most reported research on impact in composite structures concentrates on impact damage modelling from rigid body projectiles. However, soft body projectiles such as gelatine or ice are highly deformable on impact and flow, spreading the impact load and causing a pressure pulse in the structure. For reliable damage prediction in composite structures it is thus necessary to extend modelling techniques and derive appropriate data for these deformable projectiles. Ice impact in composite plates has been studied both experimentally and theoretically by Kim and Kedward [9]. They used an elastic–plastic ice model with solid finite elements for the ice projectiles. However, solid elements were found to be unsuitable in the current work on bird and gelatine impacts due to excessive element distortion which led to numerical instabilities. In [3] it is described how these soft projectiles are modelled by an alternative smooth particle hydrodynamic (SPH) method, in which the FE mesh is replaced by interacting discrete particles. Data from pressure pulses measured during gelatine and ice impact on rigid plates are used to determine parameters for the material equation of state for use with the SPH method.

Materials law and EOS for impactor

In order to use the SPH method for soft body impact simulations a constitutive law is required with suitable materials parameters. A number of materials constitutive laws have been implemented in the PAM-SHOCK SPH solver [6], mainly suitable for materials such as metals and explosives used in ballistic impact and hypervelocity impact conditions. None of which are directly relevant to the gelatine and ice impactor materials of interest here. One model currently available in PAM-SHOCK is referred to as an ''elastic–plastic hydrodynamic solid'' and was originally developed for ballistic impact in metals, which behave as isotropic elastic–plastic materials at low pressures, with an equation of state (EOS) describing the ''hydrodynamic'' pressure–volume shock behaviour at high pressures. The application of this model for gelatine impactors was described in [3], in which the elastic–plastic contribution to the materials behaviour was neglected so that the model reduced to the EOS. This simplification was valid because gelatine has very low compression strength compared with the impact pressures experienced, so that on impact the material flows immediately with negligible elastic strain energy or dissipated plastic work. This is not the case for ice, since as shown in DLR tests [10] typical compression strengths were in the range 2–10 MPa for ice and measured peak contact pressures in the HVI tests are estimated in the range 7–25 MPa. Thus the elastic–plastic contribution to the constitutive law can no longer be neglected.

The assumed materials law has the following form, where $\boldsymbol{\sigma}$ is the stress tensor and $\boldsymbol{\varepsilon}$ the total strain tensor, assumed to be made up of elastic and plastic components $\boldsymbol{\varepsilon} = \boldsymbol{\varepsilon}^e + \boldsymbol{\varepsilon}^p$. In terms of the bulk modulus K and shear modulus G, the initial isotropic elastic behaviour of the material is described by:

$$\boldsymbol{\sigma} = (K - 2G/3)(\mathrm{tr}\ \boldsymbol{\varepsilon}^e)\boldsymbol{I} + 2G\boldsymbol{\varepsilon}^e, \tag{8}$$

where $\boldsymbol{I}$ is the unit tensor. On introducing the deviatoric stress $\boldsymbol{s}$ and the deviatoric strain $\boldsymbol{e}$

$$\boldsymbol{s} = \boldsymbol{\sigma} - (1/3)(\mathrm{tr}\boldsymbol{\sigma})\boldsymbol{I}, \quad \boldsymbol{e} = \boldsymbol{\varepsilon} - (1/3)(\mathrm{tr}\ \boldsymbol{\varepsilon})\boldsymbol{I}, \tag{9}$$

eq. (8) may be decomposed into the deviatoric and dilatational components:

$$\boldsymbol{s} = 2G\boldsymbol{e}^e \quad \mathrm{tr}\ \boldsymbol{\sigma} = 3K\ \mathrm{tr}\ \boldsymbol{\varepsilon}^e. \tag{10}$$

Outside the elastic domain a plastic strain hardening function is defined as a relation between the effective plastic stress σ and effective plastic strain ε_p, defined as

$$\sigma = \left[\frac{3}{2}\mathrm{tr}\ \boldsymbol{s}^2\right]^{1/2} \quad \varepsilon_p = \int_0^t \left[\frac{2}{3}\mathrm{tr}\ (\dot{\boldsymbol{\varepsilon}}^p)^2\right]^{1/2}. \tag{11}$$

The functional form of this relation may be determined from tensile stress-strain data and is usually monotonic

increasing, up to fracture. The input data for the model are the elastic constants and a form for the plastic hardening function. This is a standard elastic–plastic materials law, which is valid at normal pressures. In this form the plastic strain is purely deviatoric, and the volume strain is purely elastic, that is tr $\boldsymbol{\varepsilon}^{\mathrm{p}} = 0$.

However under shock loading conditions, local pressures may be high and the dilatational part of the constitutive equation is replaced by an equation of state (EOS) for the pressure p, which is assumed in this case to have the polynomial form:

$$p = C_0 + C_1\mu + C_2\mu^2 + C_3\mu^3, \quad \mu = \rho/\rho_0 - 1, \tag{12}$$

where C_0, C_1, C_2 and C_3 are materials constants and μ is a dimensionless parameter defined in terms of the ratio of current density ρ to initial density ρ_0. In order to use the SPH model for the ice and concrete impactors suitable values are required for the constants C_{i} in the polynomial EOS. Since these constants refer to the dynamic behaviour of materials at impact pressures they are usually determined from shock tube or flyer plate impact tests. As the DLR is not able to measure them directly they were determined indirectly from literature information and simulations.

It is useful to relate the EOS to the elastic materials law. This follows using the definition of pressure p and compressibility parameter μ

$$p = -(1/3)(\mathrm{tr}\ \boldsymbol{\sigma}) \quad \mu = -\mathrm{tr}\ \boldsymbol{\varepsilon} = -\mathrm{tr}\ \boldsymbol{\varepsilon}^{\mathrm{e}}, \tag{13}$$

which when substituted in $(10)_2$ gives for the elastic dilatational equation:

$$\sigma = K\mu. \tag{14}$$

It follows from comparison of (12) and (14) that for elastic materials C_0=0 is the equilibrium pressure, and that C_1=K, the elastic bulk modulus. Thus the EOS is a nonlinear generalisation of the dilatational part of the elastic law (9), which is required at high pressures when the material compressibility μ is higher.

Data are now required on the additional materials parameters C_2 and C_3 in (12). Wilbeck [11] measured impact pressures of several soft body impactor materials, including rubber, gelatine and chickens and found that pressure pulses have a characteristic form which is not very sensitive to the materials properties. This consists of a short high pressure pulse caused by shock wave propagation in the impactor, followed by a lower fairly constant pressure due to steady flow of the impactor onto the target. For many materials which exhibit the linear Hugoniot relation between shock velocity v_{S} and particle velocity v_{P}:

$$v_{\mathrm{S}} = c_0 + kv_{\mathrm{P}}, \tag{15}$$

where k is a materials constant and c_0 the sound speed in the material, Wilbeck shows that the pressure–density relation across a shock has the general form

$$\rho_0 c_0^2 \eta/(1 - k\eta)^2, \text{ where } \eta = 1 - \rho_0\ \rho = \mu/(1 + \mu). \tag{16}$$

On expanding (16) for small and moderate values of μ it was shown in [3] that this takes the form of the polynomial EOS (12) with:

$$C_0 = 0, \quad C_1 = \rho_0 c_0^2,$$
$$C_2 = (2k - 1)C_1, \quad C_3 = (k - 1)(3k - 1)C_1. \tag{17}$$

It follows again that C_1 is equal to the bulk modulus of the impactor material, since C_0 is the bulk wave velocity. On assuming a linear shock Hugoniot relation, the data required for the polynomial EOS reduce therefore to the bulk modulus (or sound speed) and the Hugoniot gradient parameter k. For the synthetic bird models discussed in [3] shock data on water were used to give an estimate of k in (17).

The procedure adopted here for the ice projectile models is to make use of the quasi-static compression test data for the ice elastic/plastic materials parameters, augmented by literature data on these materials. An elastic/plastic hailstone impactor model is proposed in [9], where typical ice data may also be found. The bulk moduli of ice can be estimated fairly well from the measured compression Young's moduli. As a reasonable estimate the parameter k determined from shock tests on water may be used as an estimate for shock propagation in ice. This information is used as the basis of the procedure to calibrate the SPH model for ice a by finding suitable values of ρ_0, c_0 and k to represent the EOS of ice which fit the impact pulse data measured by the DLR in [10]. Note that in synthetic bird models, only the EOS model is required since the elastic–plastic contribution is negligible. Thus, calibration of the model is simpler in this case than for solid impactors such as ice.

Validation of soft body impactor models

Validation of the SPH synthetic bird gelatine model with the EOS by simulation of measured gas gun impact pulses on a rigid wall was presented in [3]. Here a similar procedure is used to validate an ice projectile model under impact. A series of ice impact tests were carried out in which ice cylinders were fired at speeds in the range 50–155 m/s onto a stiff metal plate mounted on a ring load

cell, which measured the resultant normal impact force–time response. Figure 2 shows the impact of an ice cylinder length 45 mm, diameter 22 mm at 155 m/s on the load cell target plate. An FE model was developed for the ring force transducer, the circular aluminium target plate, with an SPH mesh containing about 1,000 particles for the ice cylinder. Figure 3 shows that the particle model simulates well the fracture and flow behaviour of the ice over the target plate on contact during high velocity impact. A quantitative validation of the ice impactor model is obtained by comparison of measured and predicted normal force pulses on the load cell, as shown in Fig. 4. The test data shown correspond to a 17 g ice projectile impacting the plate at 155 m/s. It is seen that the pulse shapes are in good agreement, with initial peak forces of about 18 kN well predicted by the ice impactor model, although the simulated pulse width was shorter than the test pulse. The agreement is considered reasonably good as an initial basis for structural impact simulations with ice impactors. Further improvements to the ice constitutive law are required to understand temperature effects, which influence the elastic/plastic response quite significantly, and to include correctly tensile brittle fractures which are not well represented in the current model.

FE simulation of soft body impact on composite structures

Validation of the code developments with the composites shell damage and delamination models for rigid impactors and with the SPH soft body impactor models are reviewed in [5]. For soft body impacts a gas gun test programme was carried out at the DLR in which idealised composite shells,

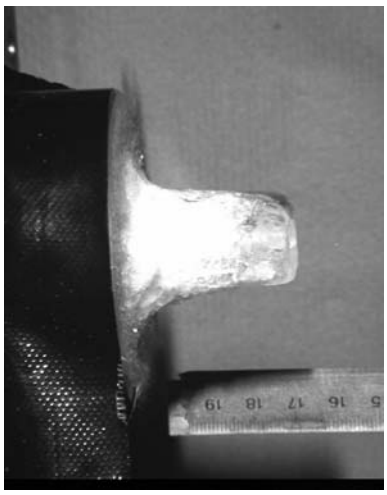

Fig. 2 Deformation and failure of ice cylinder projectile impacting load cell at 97.2 m/s

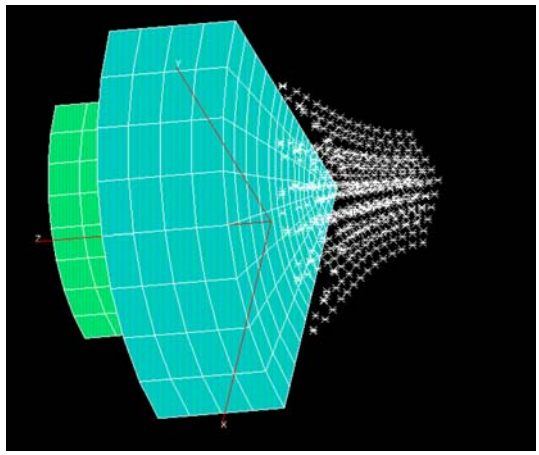

Fig. 3 SPH model of ice projectile deformation during impact on load cell (quarter model, M = 12 g, V_0=150 m/s)

typical of a wing leading edge (LE) profile, were tested with gelatine cylinder projectiles with masses in the range 30–34 g at 132.5–198 m/s normal impact. At the higher velocities there was extensive delamination in the structures and some fibre fracture at the contact region. FE simulation results of the impact damage in these idealised structures were presented in [3], using the CDM ply failure models with delamination interfaces, and showed satisfactory agreement with the observed impact damage. The ice model described above has been used to simulate ice impact damage in composite sandwich panels in the EU CRAHVI project [12] and is currently being applied to assess novel sandwich fuselage structures in an ongoing DLR project with Airbus. Predictions with the model are satisfactory but are not yet ready for publication. For high velocity impacts quantitative load pulse data to compare with simulated results are difficult to obtain, however qualitatively there is good agreement with observed deformations and damage conditions. Impact from soft body impactors reduces the likelihood of local penetration failure and fibre fracture seen in rigid projectile tests, hence

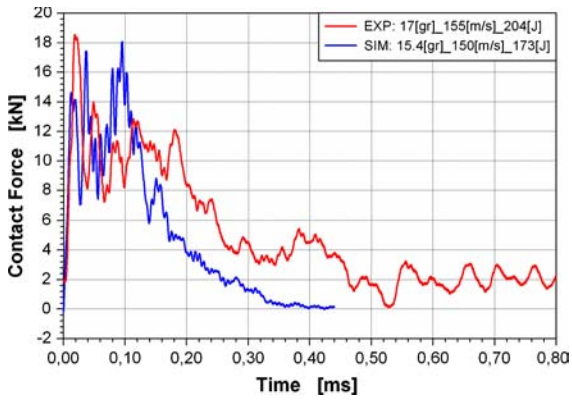

Fig. 4 FE simulation of ice projectile test—comparison of test and simulated pulses

energy absorption mechanisms due to delamination become more important with impact energy stored as strain energy in large shell bending deformations. Results have shown that a simulation technique with an SPH impactor model and shell or stacked shell structural models is very promising for simulating soft body impacts in composite structures.

In the EU CRAHVI project [12] the methods were thus applied in a design study to evaluate a leading edge concept structure under synthetic bird impact, which is now summarised here. The objective was to evaluate design concepts for a composite wing LE with improved energy absorption under bird impact. In the tensor skin LE concept developed by NLR and described in more detail in [13], the skin structure contains loops of ductile composite plies which are designed to unfold at bird impact to load the ribs in-plane. The ribs then absorb bird strike energy, limiting the impact load on the structure behind. Details of lay-up of the fabricated structure NLR-LE-2 are listed in Table 1. The LE composite shell laminate consists of three composite sublaminates: the cover laminate as protective outer skin in aramid fabric/epoxy; the carrying laminate, a load bearing inner laminate of carbon/aramid hybrid fabric/epoxy and the tensor laminate, an energy absorbing middle laminate composed of folded Dyneema fabric/epoxy. In addition there is a protective strip laminate at the rib/shell connections. On impact the relatively brittle outer and inner skins are designed to fracture and the bird is captured by the tensor laminate which unfolds, making large deformation and hence energy absorption possible, before it is loaded to failure. Dyneema layers consist of fabric plies made from high performance polyethylene fibres, which have high tenacity and are used in ballistic protection devices. Dyneema/epoxy has lower stiffness and strength but higher failure strains than carbon or glass epoxy composites, which allows the tensor laminate to unfold and absorb mechanical energy by large deformation tension loads. NLR fabricated three such structures for bird impact testing in the CRAHVI project. DLR bird impact simulation studies described here were on the structure NLR-LE-2 which was impact tested in a gas gun facility at CEAT under conditions of normal impact with 1.8 kg synthetic bird, between the ribs at 97.2 m/s, [13]. The impact point was at the apex of the LE along the centre line and impact direction was normal to the backing plate. The test condition represents a typical landing speed of a commuter aircraft when bird impacts are likely and where the LE is required to absorb bird energy to prevent damage to the wing spar.

Figure 5 shows the FE model developed for the bird simulation on the LE structure. A detailed FE model with the tensor skin laminate is used for the central shell impact region of the LE between the two inner ribs. The complete model has a length 850 mm and contains four ribs. The main aim of the bird impact tests is to demonstrate the tensor unfolding concept for increasing shell energy absorption, so that rib deformation with additional energy absorption was not considered desirable in the tests. Thus the ribs in the test structures were fabricated from 10 mm thick aluminium plates, and the end ribs were tied to the base plate to prevent lateral movement. In the tests the ribs behaved as rigid plates and were undamaged so that in the model the ribs were assumed to be rigid bodies with the LE shell laminate fixed at the points of contact with the curved rib edges. The steel backing plate was modelled, with an assumption that the LE is fixed at its longitudinal edges to the steel plate, and that the four ribs are fixed to the backing plate. The backing plate was mounted on a rectangular steel box beam frame structure. Figure 5 also shows the SPH model representing a 1.8 kg synthetic bird. For the DLR bird model an impactor geometry was specified as a solid cylinder with two hemispherical end caps, with cylinder length 114 mm, diameter 114 mm, and end cap radius 57 mm. A solid FE mesh was adopted for the impactor which when converted to a particle mesh consisted of 4,320 uniformly spaced particles in a quarter model bird model. The polynomial EoS was used to describe the behaviour of the gelatine material, with constants C_i defined in (12).

Figure 6 shows details of the laminate FE stacked shell model containing cover laminate, tensor laminate with embedded loops, and carrying laminate, which is used for the central impacted region of the LE between the inner ribs. Note that NLR-LE-2 contains a three loop tensor concept, as discussed in [13], and this can be seen in Fig. 6. The cover laminate, tensor laminate and carrying laminate are each modelled in PAM-CRASH as single layered shell elements, which are connected through their thickness by contact interfaces. These are shell-to-shell cohesive interfaces with failure. They allow a through-thickness tension/

Table 1 Lay-up of LE concept structure

Specimen	Sublaminate	Lay-up	Laminate ID
NLR-LE-2	Dyneema SK65 fabric	$\{[0]_2\}_3$	Tensor
	Carbon/aramid hybrid prepreg	[45, 0, 90, 0, 45]	Carrying
Length: 850 mm	Aramid/epoxy prepreg	[45]	Cover
Rib-pitch: 230 mm	Aramid/epoxy prepreg	$[45]_2$	Protection-strip (width: 40 mm)

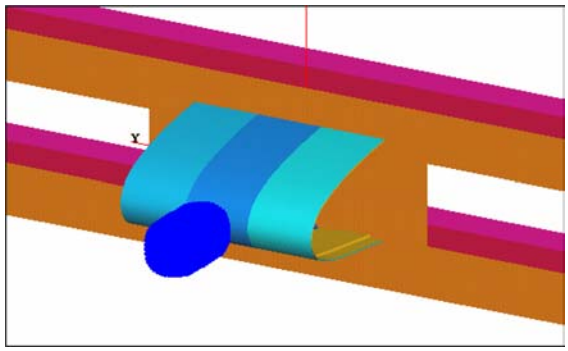

Fig. 5 FE model of LE test set-up

shear failure condition to be defined which may be governed by the delamination failure criterion discussed above, or by a simpler multiaxial fracture condition when the interface fails allowing adjacent shells to separate. This method permits separation between the cover, tensor and carrying laminates, as well as separation within adjacent elements in the folded tensor laminate. For the aramid fabric cover laminate and carbon/aramid fabric carrying laminate a layered shell Type 132 is used in PAM-CRASH, together with the bi-phase fabric Ply 6 model discussed above. The fabric ply model includes ply damage prior to failure and allows for the re-orientation of fibres under large in-plane shear deformations. A ''hybrid'' model for the tensor laminate was used, in which elastic–plastic plies are added to the brittle composite plies in an attempt to bring ductility into the model of the tensor laminate. This was necessary since DLR tests on Dyneema/epoxy laminates showed high tenacity and an almost ductile failure at high strains. The tensor laminate was modelled as a layered shell Type 131 with both bi-phase composite plies (Ply 0) and elastic/plastic plies (Ply 2). In this way it is possible to model the observed ductility in the Dyneema/epoxy laminate, allowing it to unfold without immediate fracture.

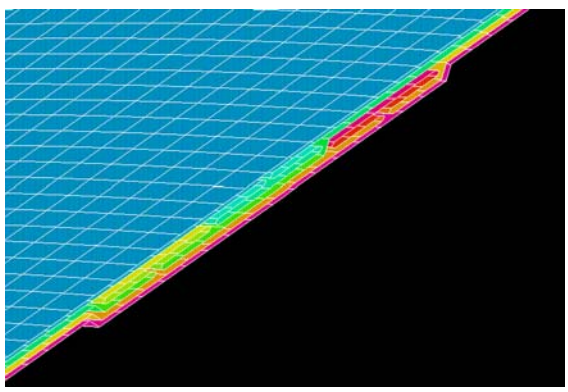

Fig. 6 Details of FE shell model for LE laminate with 3-loop tensor ply

The high speed film from the CEAT gas gun test on the LE structure [13] showed extensive damage and fracture in the cover and carry plies with unfolding of the tensor. The tensor ply was activated and unfolded absorbing the kinetic energy of the penetrating parts of the bird. The bird flowed partly around the LE and a significant bird mass was trapped in the unfolded tensor ply, as seen in Fig. 7a. The damaged LE structure after impact is shown in Fig. 8a with a large conical indentation at the impact point having a diameter about the same as the rib spacing, and a hole with fractured fibres at the apex. The FE simulation results agreed well with the observed failure behaviour in the test. The SPH bird flows round the LE and also fractures the cover ply and penetrates into the tensor laminate, as seen in Fig. 7b. Note that this complex flow and separation behaviour cannot be modelled by a bird model using solid FE elements. Figure 8b shows the predicted damaged LE after impact in the central region containing the tensor laminate. Simulation results show clearly the damage and element elimination of much of the cover ply, the unfolding of the tensor ply and the large deformation and penetration of the carry ply. Simulated damage in Fig. 8b should be compared with the post-test photograph of the LE from CEAT presented in Fig. 8a. Note that computed displacement contours gave a maximum penetration of about 60 mm, which agrees well with the observed damage. More detailed comparisons of strain gauge data and resultant force pulses on the backing frame structure were carried out to further validate the simulation methodology.

Conclusions

The paper has described recent progress on materials modelling and numerical simulation of soft body impact on fibre reinforced composite structures. The work is based on the application of explicit finite element (FE) analysis codes to simulate composite shell structures under impact from highly deformable soft impactors such as gelatine or ice, which may flow over the structure spreading the impact load. These soft impactors are modelled here by the smooth particle hydrodynamic (SPH) method, in which the FE mesh is replaced by interacting particles. It is very difficult to measure the impactor properties under relevant dynamic load conditions for use in the SPH model. The method adopted was to calibrate the parameters required for the EOS by simulating gelatine and ice impacts on rigid targets and comparing geometrical flow characteristics and pressure or force pulses observed with simulation results.

In high velocity impact of soft bodies on composite structures both delamination and ply failures are found to be important, depending on the impact energy levels. A composites failure model which includes ply damage and in-

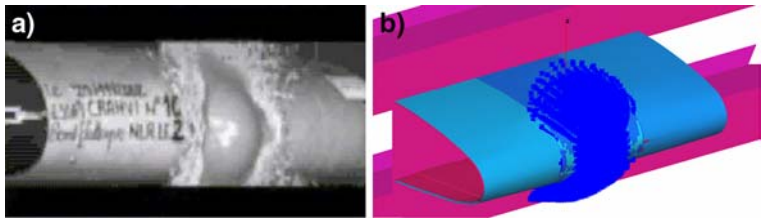

Fig. 7 Impact simulation of LE under impact from 1.82 kg synthetic bird at 97.2 m/s. (**a**) LE during impact (Courtesy CEAT [13]). (**b**) Bird impact simulation at 2.4 ms

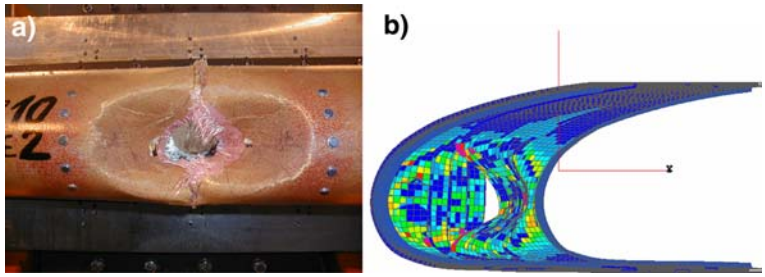

Fig. 8 Damage in LE after bird impact. (**a**) Damaged LE (Courtesy CEAT [13]). (**b**) FE simulation of damage in carry ply

terply delamination model has been developed and was used here to predict impact damage in the shell structures. Numerical simulations using the SPH impactor model with the improved composites failure model have been compared in earlier work with gelatine and ice impact test data on composite shell structures and gave encouraging results. Here the methods were applied to a concept study for a novel LE concept structure designed for improved energy absorption under bird impact. The failure behaviour of the LE is based on unfolding and subsequent failure of a ductile Dyneema/epoxy sublaminate within a more brittle carbon and aramid/epoxy shell laminate. There was encouraging qualitative and quantitative agreement between the gas gun impact test and the FE simulations of the failure behaviour. Simulation and test suggest that 100 m/s is a critical impact velocity for this structure for a 1.82 kg synthetic bird. In simulations at lower impact velocities of 80 m/s the bird flowed over the LE and only minor damage occurred, whilst at 100 m/s the LE structure was significantly damaged with the tensor laminate unfolding to absorb bird kinetic energy and prevent possible damage to the wing spar.

Results have shown that the simulation methodology developed here with an SPH impactor model and shell or stacked shell structural models is very promising for simulating soft body impacts in composite structures. Further work is required to improve composites damage models by including effects of damage mode interactions and rate dependence. Future developments which are important in aircraft safety studies include improvements to enhance the robustness of explicit FE codes, multiscale methods to allow detailed local damage models to be interfaced with larger scale models of aircraft structures, and improved models of foreign objects such as birds, hailstones, burst tyre fragments, and runway debris under dynamic failure conditions.

Acknowledgements Some of the work presented was developed in the EU project CRAHVI [12]. The authors wish to acknowledge financial support from the CEC and the CRAHVI partners for their valuable collaboration.

References

1. Ladevèze P (1994) In: Talreja R (ed) Damage mechanics of composite materials, Composite Materials Series 9, Chapter 4. Elsevier, Amsterdam
2. Johnson AF, Pickett AK, Rozycki P (2001) Composites Sci Technol 61:2183
3. Johnson AF, Holzapfel M (2003) Composite Struct 61:103
4. Ladevèze P, Le Dantec E (1992) Composites Sci Technol 43:257
5. Johnson AF (2005) In: Beaumont P and Soutis C (eds) Multiscale modelling of composite materials and systems, Chapter 14. Woodhead, Cambridge
6. PAM-SHOCK™/PAM-CRASH™ FE Code. Engineering Systems International, F-94513 Rungis Cedex, France
7. Allix O, Ladevèze P (1992) Composites Struct 22:235
8. Crisfield MA, Mi Y, Davies GAO, Hellweg HB (1997) In: Owen DRJ et al (eds) Computational plasticity – fundamentals and applications', Part 1. pp 239–254
9. Kim H, Kedward KT (1999) Experimental and numerical analysis correlation of hail ice impacting composite structures. 40th AIAA Structures, Structural Dynamics and Materials Conference, St Louis, AIAA-99-1366
10. Holzapfel M, Johnson AF, Kraft H, Reiter A (2002) CRAHVI D5.4.3: ice impact tests. DLR Report, DLR-IB, 435-2002/5
11. Wilbeck JS (1977) Impact behaviour of low strength projectiles. Air Force Materials Laboratory, Technical Report AFML-TR-77-134
12. CRAHVI: Crashworthiness of Aircraft for High velocity Impact, CEC Project: G4RD-CT-2000-00395, 2001–2004
13. Ubels L, Johnson AF, Gallard J, Sunaric M (2003) Design and testing of a composite bird strike resistant leading edge. Proceedings of the 24th International SAMPE Europe conference, Paris